CALPHAD: Computer Coupling of Phase Diagrams and Thermochemistry ▮ (▮▮▮▮) ▮▮▮–▮▮▮

Contents lists available at ScienceDirect

CALPHAD: Computer Coupling of Phase Diagrams and Thermochemistry

journal homepage: www.elsevier.com/locate/calphad

A thermodynamic description of the Al–Ca–Zn ternary system

S. Wasiur-Rahman, M. Medraj *

Department of Mechanical and Industrial Engineering, Concordia University, 1455 De Maisonneuve Blvd. West, Montreal, QC, Canada, H3G 1M8

ARTICLE INFO

Article history:
Received 10 February 2009
Received in revised form
10 June 2009
Accepted 11 June 2009
Available online xxxx

Keywords:
Al–Zn
Al–Ca
Al–Ca–Zn
Modified quasichemical model
Thermodynamic modeling

ABSTRACT

A comprehensive thermodynamic database of the Al–Ca–Zn ternary system is presented for the first time. Critical assessment of the experimental data and re-optimization of the binary Al–Zn and Al–Ca systems have been performed. The optimized model parameters of the third binary system, Ca–Zn, are taken from the previous assessment of the Mg–Ca–Zn system by the same authors. All available as well as reliable experimental data both for the thermodynamic properties and phase boundaries are reproduced within experimental error limits. In the present assessment, the modified quasichemical model in the pair approximation is used for the liquid phase and Al_FCC phase of the Al–Zn system to account for the presence of the short-range ordering properly. Two ternary compounds reported by most of the research works are considered in the present calculation. The liquidus projections and vertical sections of the ternary systems are also calculated, and the invariant reaction points are predicted using the constructed database.

1. Introduction

In order to form complex shaped structures, the superplasticity method is regarded as a viable technique.The technique has the advantages of delivering exceptional formability and potentially giving good dimensional tolerance [1]. Al-based alloys have long standing as a work metal for superplastic applications due to their lightness and superior creep properties compared with those of the standard zinc-based alloys [2]. The Al–Zn eutectoid alloy and the Al–$CaAl_4$ eutectic alloy are known to be superplastic. However, sheets made of these alloys are brittle and cannot be cold rolled industrially, whereas Al alloys containing Ca and Zn are more ductile and can be cold rolled to superplastic sheets using conventional rolling systems [3]. In addition, the Al–Ca–Zn ternary system is an integral part in the family of the Mg–Al–Ca–Zn quaternary system in which two other ternary systems, Mg–Al–Ca [4] and Mg–Al–Zn [5–8], have been well described in terms of thermodynamic modeling in the literature, and recently the present authors remodeled the Mg–Ca–Zn ternary system [9].

Despite the high potential of the Al–Ca–Zn alloy system in cutting-edge technology applications, no conclusive work regarding thermodynamic modeling of the phase equilibrium could be found in the literature. Hence, it was decided, in the present work, to model the system based on the CALPHAD method [10]. All three constituent binary systems Al–Zn, Ca–Zn and Al–Ca were optimized in the past; the previous optimizations [11–15] of the Al–Zn binary system were done without considering the presence of short-range ordering (SRO) in the liquid phase as well as in the Al_FCC solid solution phase of Al–Zn system. Even though the recent optimization [16] on Al–Ca system considered short-range ordering in the liquid phase through the modified quasichemical model (MQM), their calculation [16] shows some deviation from the experimental results in the key invariant points. Hence, the Al–Zn and Al–Ca binary systems will be re-optimized and the Al–Ca–Zn ternary system will be optimized for the first time in the present assessment. The modified quasichemical model (MQM) was employed for the liquid phase and Al_FCC phase of the Al–Zn binary system to account for the presence of short-range ordering. Two ternary compounds reported by Ganiev et al. [17] and Gantsev et al. [18] were considered during modeling of the Al–Ca–Zn system in the present work after careful assessment of the different contradicting experimental results from the literature regarding the number and type of ternary compounds in the system. The optimized model parameters of the Ca–Zn binary system will be taken from the authors' previous assessment [9]. All the thermodynamic optimization and calculation of the present study have been performed using FactSage 5.5 software [19].

2. Literature review of the experimental results

The initial step of thermodynamic modeling and optimization according to the CALPHAD method is to collect and classify experimental data relevant to the Gibbs energy as input. Crystallographic information is also useful for modeling the Gibbs energy, especially

* Corresponding author. Tel.: +1 514 848 2424x3146; fax: +1 514 848 3175.
E-mail address: mmedraj@encs.concordia.ca (M. Medraj).
URL: http://www.me.concordia.ca/~mmedraj (M. Medraj).

0364-5916/$ – see front matter © 2009 Elsevier Ltd. All rights reserved.
doi:10.1016/j.calphad.2009.06.001

Table 1
Crystallographic information for all the solid phases in the Al–Ca–Zn ternary system.

Phase	Structure type	Pearson symbol	Space group	Model[a]	Note	Reference
HCP	$A3$	$hP2$	$P6_3/mmc$	RM	Zn has stable HCP phase	[80]
FCC	$A1$	$cF4$	$Fm\bar{3}m$	MQM, RM	Al, Ca have stable FCC phase	[80]
BCC	$A2$	$cI2$	$Im\bar{3}m$	RM	Ca has stable BCC phase	[80]
Al_4Ca	$D1_3$		$I4/mmm$	ST		[81]
Al_2Ca	$C15$		$Fd3m$	ST		[81]
$Al_{14}Ca_{13}$	Monoclinic		$C2/m$	ST		[81]
Al_3Ca_8	Triclinic		P	ST		[81]
Ca_3Zn	$E1_a$	$oC16$	$Cmcm$	ST		[82]
Ca_5Zn_3	$D8_1$	$tI32$	$I4/mcm$	ST		[83]
CaZn	B_f	$oC8$	$Cmcm$	ST		[82]
$CaZn_2$		$oI12$	$Imma$	ST		[84]
$CaZn_3$		$hP32$	$P6_3/mmc$	ST		[82]
$CaZn_5$	$D2_d$	$hP6$	$P6/mmm$	ST		[85]
$CaZn_{11}$		$tI48$	$I4_1/amd$	ST		[86]
$CaZn_{13}$	$D2_3$	$cF112$	$Fm3c$	ST		[87]
$CaAl_2Zn_2$	Tetragonal	$tI10$	$I4/mmm$	ST		[69]
CaAlZn				ST	No information available	

[a] RM = Random mixing, MQM = Modified Quasichemical Model, ST = Stoichiometric compound.

for the ordered phases. The list of crystallographic information for all the phases considered in the present study is given in Table 1. The next step is to critically evaluate the collected experimental data by identifying the inconsistent and contradicting results and choosing the most reliable sets to be used for optimization [20].

2.1. Al–Zn binary system

Heycock and Neville [21] first investigated the system using thermal analysis. They [21] determined the liquidus curve with the eutectic point occurring at 653.5 K and 89 at.% Zn whereas the values of Tanabe [22] and Isihara [23] were 658 K at 88.7 at.% Zn and 653 K at 88.7 at.% Zn, respectively. Tanabe [22] studied the system by means of thermal analysis, microstructure and electrical resistance methods to determine the liquidus and Al-solidus curve. The Al-solidus curve of Tanabe [22] was not considered in the present work due to the fact that he did the experiment by keeping the samples in the melt tube, so the phase change determination cannot be accurate enough, and this was pointed out by Isihara [23], who also used the same methods as Tanabe [22] supplemented by the dilatometric method and X-ray diffraction analysis. From Isihara [23], the averages of the heating and cooling curves were chosen in the present calculation because of the discrepancy between heating and cooling that was acknowledged by the author himself. Gayler et al. [24], also, determined the liquidus and Al-solidus curve using thermal and microscopic analyses. The experimental results of Gayler et al. [24] agree fairly well with those of Pelzel and Schneider [25], who studied the system from 30 to 100 at.% Zn using the specific volume method.

The liquidus curve was also studied by Butchers and Hume-Rothery [26], Pelzel [27], Solet and Clair [28] and Peng et al. [29]. The results of [26–28] agree fairly well with each other; all of them used thermal analysis. In contrast, Peng et al. [29] used an acoustic emission method; they reported a higher liquidus temperature than the previous researchers.

The Al-solidus curve was also investigated by several researchers. Among them, Morinaga [30] and Gebhardt [31] used microscopic analysis, Ellwood [32] used high-temperature X-ray diffraction and Araki et al. [33] used electron-probe microanalysis (EPMA) in order to determine the solidus line. Early works of Tanabe [22] and Isihara [23] showed lower values for the solidus temperatures and they found a series of thermal arrests between 713 K and 720 K, which they [22,23] attributed to a peritectic reaction, L + (Al) $\leftrightarrow$ solid solution (β). Later, Gayler et al. [24] and Morinaga [30] demonstrated that this thermal effect is the result of segregation. They [24,30] found no evidence of any kind of phase change, and this was supported by later investigators such as Ellwood [32] and Fink and Willey [34].

The FCC miscibility gap has also been studied by numerous groups of investigators [32,34–36]. Fink and Willey [34] used electrical resistivity at elevated temperature and found two aluminum solid solutions in equilibrium at a temperature above 548 K. According to Fink and Willey [34], the critical temperature is 626 K at 38.5 at.% Zn. Borelius and Larsson [35] and Munster and Sagel [36] also used electrical resistivity measurements to determine the miscibility gap. The miscibility gap was also studied by Ellwood [32], who used high-temperature X-ray diffraction. Larsson [37] also determined the boundary of the miscibility gap using electrical resistivity measurements on 28 different Al–Zn alloys in the composition range 1 to 65 at.% Zn. The results of Larsson [37] show slightly higher temperatures in comparison with the values of [32,34,36] above 50.0 at.% Zn. After that, X-ray diffraction and transmission electron microscopy were used by Simerska and Bartuska [38] to measure the Al solvus line and boundary of the miscibility gap up to 30.0 at.% Zn, and their results [38] were consistent with the experimental works of Ellwood [32], Fink and Willey [34], Borelius and Larsson [35] and Munster and Sagel [36]. Moreover, Terauchi et al. [39] reported the critical temperature to be 624 K at 39.16 at.% Zn and eutectoid temperature as 548 K using the small-angle X-ray scattering method and cooling curve technique. The reported eutectoid temperature of Terauchi et al. [39] is close enough to the later investigation of Holender and Soltys [40], who used an electrical resistivity method and reported this value as 549 K. Peng et al. [29] also studied the miscibility gap using an acoustic emission method, and their results agree well with the earlier experimental works of Ellwood [32], Fink and Willey [34], Borelius and Larsson [35], Munster and Sagel [36] and Simerska and Bartuska [38].

The solubility of Zn in Al was determined by Tanabe [22], Fink and Willey [34], Borelius and Larsson [35], Ellwood [32] and Araki et al. [33]; the results were more or less consistent with each other except in the composition range 10 to 16.5 at.% Zn. The data of Tanabe [22], Fink and Willey [34] and Borelius and Larsson [35] for the phase boundary Al_FCC$_2$/(Al_FCC + Zn_HCP) are consistent in the range 59 to 67 at.% Zn, whereas the data of Larsson [37] show more scatter than the results of [22,34,35].

The experimental works of most of the researchers [41,42,44–46] regarding the solubility of Al in Zn are in good agreement with each other. At first, Peirce and Palmerton [41] measured the solubility of Al in Zn using electrical resistivity measurements supplemented by microscopic analysis. Then Auer and Mann [42] used magnetic susceptibility to measure the

Please cite this article in press as: S. Wasiur-Rahman, M. Medraj, A thermodynamic description of the Al–Ca–Zn ternary system, CALPHAD: Computer Coupling of Phase Diagrams and Thermochemistry (2009), doi:10.1016/j.calphad.2009.06.001

same phenomena. Lattice parameters were measured by Fuller and Wilcox [43], Burkhardt [44], Lohberg [45] and Hofmann and Fahrenhost [46], to detect the Zn solvus line. However, the data of Fuller and Wilcox [43] will not be considered in the present assessment because the alloy samples were not made from pure Al and Zn and there was uncertainty in the temperature measurements especially at elevated temperature. Afterward, Pasternak [47] made measurements using electrical resistivity and they confirmed the earlier results of Peirce and Palmerton [41], Auer and Mann [42], Burkhardt [44], Lohberg [45] and Hofmann and Fahrenhost [46].

Similar to phase equilibrium studies, a large number of experimental works investigating the thermodynamic properties both for the liquid phase as well as for the extended solid solution of the Al_FCC phase have been found in the literature. Enthalpy of mixing over the liquid Al–Zn alloys was performed by Wittig and Keil [48] calorimetrically at 953 K. The same property for the Al_FCC phase was measured by Hilliard et al. [49], Corsepius and Munster [50], Wittig and Schoffl [51] and Connell and Downie [52]; the former two investigators [49,50] used EMF measurements at 653 K and the latter two [51,52] used solution calorimetry at 643 K and 637 K, respectively. Poor agreement has been found between the calorimetric data and those from EMF studies, particularly in the composition range 0 to 40 at.% Zn. Although the agreement is better around 40 at.% Zn, the trends in composition of the two sets of data are quite different.

The activity of Al in the Al–Zn liquid alloys was measured by Batalin and Beloborodova [53] at 960 K, Predel and Schallner [54] at 1000 K and 1100 K and Sebkova and Beranek [55] at 973 K and 1073 K. All of them used the EMF method and their results agree fairly well with each other. The activity of Zn in the liquid phase was determined by Lutz and Voigt [56] at 1000 K, Bolsaitis and Sullivan [57] at 1076 K, and later by Yazawa and Lee [58] at 1073 K. Both Lutz and Voigt [56] and Yazawa and Lee [58] measured the vapor pressure over a number of liquid alloys using the dew point method, whereas the activity of Zn was determined by Bolsaitis and Sullivan [57] using the isopiestic technique.

The activity of Al in the solid Al_FCC phase was measured by Ptak and Zabdyr [59] and Miller et al. [60] using the EMF method at 653 K and 703 K, respectively, while that of Zn was determined by Piacente et al. [61] through measuring the partial pressure of Zn using a multiple rotating Knudsen source coupled with a mass spectrometer at 660 K, and by atomic absorption by Takahashi and Asano [62] at 653 K. Earlier, both Hilliard et al. [49] and Corsepius and Munster [50] measured the partial Gibbs energy of Al in the FCC solid solution phase at 653 K using the EMF method; their results show reasonable agreement with each other and will be used in the present work. In addition, Hilliard et al. [49] determined the partial enthalpy of Al in the solid phase at 653 K.

The thermodynamic and phase equilibrium data were critically assessed by Murray [11]. However, the calculated phase diagram was not in good accord with the experimental data available in the literature and she did not mention the types of models used for the different phases. Mey and Effenberg [12] subsequently re-evaluated this system thermodynamically, but their calculated phase boundaries of Al_FCC$_2$/(Al_FCC + Zn_HCP), as well as those for the miscibility gap of the FCC phase, differ markedly from the experimental values. A thermodynamic calculation of this system was carried out later by Mey [13], Chen and Chang [14] and recently by Mathon et al. [15]. However, none of the aforementioned authors considered the short-range ordering either for the liquid or for the Al_FCC solid solution phase in their calculations. All these works [12–15] used the Bragg–Williams random solution model represented by the Redlich–Kister polynomial [63] to model the liquid phase and the Al_FCC phase which cannot account for the presence of short-range ordering.

2.2. Al–Ca binary system

A few research groups [16,64,65] have worked on this system in the past performing both experimental and modeling studies. The most recent work was done by Aljarrah and Medraj [16], in which they executed a thorough critical evaluation of all the available experimental works from the literature. They [16] used the modified quasichemical model for the liquid phase in order to account the presence of short-range ordering. Some of their calculated invariant points deviate a bit from the experimental points and have been improved in the course of the present work by modifying the excess Gibbs energy parameters.

2.3. Al–Ca–Zn ternary system

A limited amount of experimental data could be found in the literature for the Al–Ca–Zn ternary system. Kono et al. [66] studied the system using micrography, inverse rate thermal analysis, X-ray diffraction and EPMA analysis. They [66] reported two quasibinary sections between Al–CaAlZn and Al–$CaZn_{13}$. But they indicated congruent melting of the compound $CaZn_{13}$ in the Al–$CaZn_{13}$ section which is known to melt incongruently in the binary Ca–Zn system. Their reported melting point for the $CaZn_{13}$ compound was higher by almost 60 K than the incongruent melting temperature reported in the literature [67,68]. They also reported two ternary compounds: CaAlZn and $CaZnAl_3$; the first one melted congruently and the latter formed by peritectic reaction from the liquid and the CaAlZn phase at 1129 K. Cordier et al. [69] determined the crystal structure of a new ternary compound $CaAl_2Zn_2$ which is different from those reported by Kono et al. [66]. Later, Prince [70] assessed the Al–Zn side of the Al–Ca–Zn system based on the work of Kono et al. [66] without mentioning the details of the thermodynamic model. After that, Ganiev et al. [17] used differential thermal analysis (DTA), X-ray diffraction and metallographic analysis to study the Al–Ca–Zn system and reported two compounds, CaAlZn and $CaAl_2Zn_2$, which undergo congruent melting. The most recent work on this system has been conducted by Gantsev et al. [18] using metallographic analysis. They [18] reported the same two ternary compounds as Ganiev et al. [17]. Hence it can be concluded that the existence of the CaAlZn ternary compound has been confirmed by most prior researchers. This compound will be included in the current optimization. On the other hand, Kono et al. [66] reported a second ternary compound, $CaZnAl_3$, which was different from $CaAl_2Zn_2$ reported by Ganiev et al. [17] and Gantsev et al. [18] in terms of composition. Moreover, the crystal structure of $CaAl_2Zn_2$ was also confirmed by Cordier et al. [69]. Therefore the $CaAl_2Zn_2$ compound will be included in the current optimization of the Al–Ca–Zn system.

3. Analytical description of the thermodynamic models employed

The Gibbs energy of pure element i (i = Al, Ca and Zn) in a certain phase ϕ is described as a function of temperature by the following equation:

$$^{0}G_i^{\phi}(T) = a + bT + cT\ln T + dT^2 + eT^3 + fT^{-1} + gT^7 + hT^{-9} \quad (1)$$

where $^{0}G_i^{\phi}(T)$ is the Gibbs energy at standard state and T is the absolute temperature. The value of the coefficients a to h are taken from the SGTE (Scientific Group Thermodata Europe) compilation by Dinsdale [71].

The Gibbs energy for stoichiometric compounds is described by the following equation:

$$G^{\phi} = x_i\,^{0}G_i^{\phi_1} + x_j\,^{0}G_j^{\phi_2} + \Delta G_f \quad (2)$$

Please cite this article in press as: S. Wasiur-Rahman, M. Medraj, A thermodynamic description of the Al–Ca–Zn ternary system, CALPHAD: Computer Coupling of Phase Diagrams and Thermochemistry (2009), doi:10.1016/j.calphad.2009.06.001

Table 2
Optimized model parameters of the liquid binary Al–Zn, Al–Ca and Ca–Zn phases.

Atom–atom "coordination numbers"[a]				Gibbs energies of pair exchange reactions (J/mol)
A	*B*	Z^A_{AB}	Z^B_{BA}	
Al	Zn	5	5	$\Delta^{ex}G^{liq}_{AlZn} = 4057.94 - 1.463T$
Al	Ca	3	6	$\Delta^{ex}G^{liq}_{AlCa} = -30572.52 + 10.58T + (1.32T)X_{AlAl} + (-4890.6 - 0.38T)X_{CaCa}$
Ca	Zn	6	3	$\Delta^{ex}G^{liq}_{CaZn} = -17765 + 0.084T - 10282.8X_{CaCa} - 7942.0X_{ZnZn}$[b]

[a] For all pure elements (A = Al, Ca and Zn), $Z^A_{AA} = 6$.
[b] Parameter taken from Wasiur-Rahman and Medraj [9].

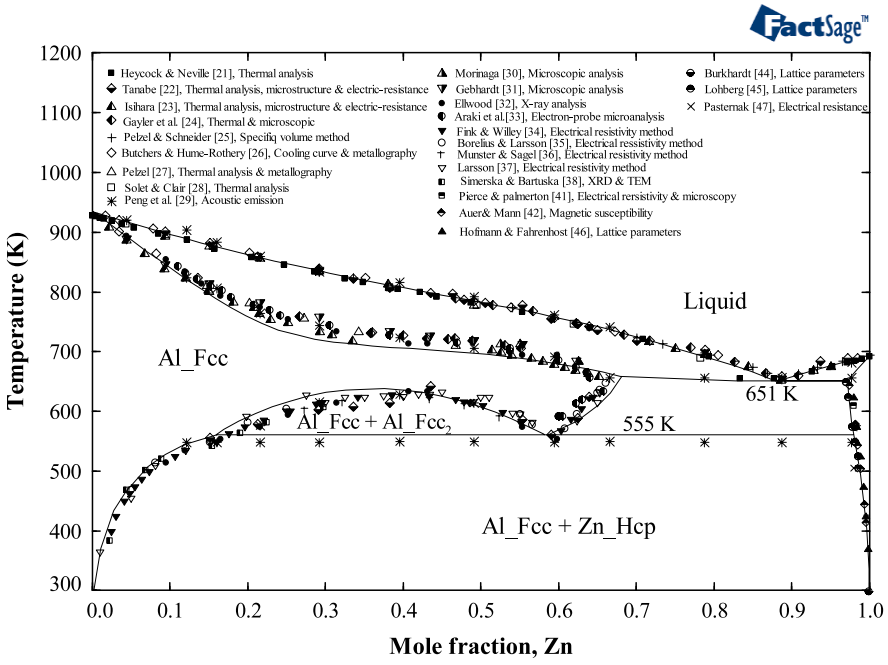

Fig. 1. Re-optimized Al–Zn phase diagram in relation to the experimental results.

Table 3
Comparison between calculated and experimental values of the invariant reactions in the Al–Zn system.

Reaction type	Reaction	Composition (at.% Zn)	Temperature (K)	Reference
		88.2	651.0	This work
		89.0	653.5	[21]
		88.7	658.0	[22]
Eutectic	L ↔ Al_FCC + Zn_HCP	88.7	653.0	[23]
		–	654.0	[24]
		88.7	653	[25]
		88.7	655	[26]
		58.3	555.0	This work
		59.8	553.0	[32]
		–	548.0	[34]
Eutectoid	Al_FCC_2 ↔ Al_FCC+Zn_HCP	–	550.0 ± 0.5	[35]
		59.4	553.0	[37]
		–	548.0	[39]
		–	549.0	[40]
		38.5	634.0	This work
Critical point	Al_FCC ↔ Al_FCC + Al_FCC_2	38.5	626.0	[34]
		39.16	624.0	[39]

where ϕ denotes the phase of interest, x_i and x_j are the mole fractions of component i and j, ${}^0G_i^{\phi_1}$ and ${}^0G_j^{\phi_2}$ represent the Gibbs energy in their standard state and $\Delta G_f = a + bT$ is the Gibbs energy of formation per mole of atoms of the stoichiometric compound, where the parameters a and b are obtained by optimization using experimental results of phase equilibria and thermodynamic data.

The random solution model was used to describe the disordered terminal solid solution phases, which can be expressed as

$$G = x_i {}^0G_i^{\phi} + x_j {}^0G_j^{\phi} + RT[x_i \ln x_i + x_j \ln x_j] + {}^{ex}G^{\phi}. \quad (3)$$

The excess Gibbs energy, ${}^{ex}G^{\phi}$, is expressed using the Redlich–Kister polynomial [63] as follows:

$${}^{ex}G^{\phi} = x_i.x_j \sum_{n=0}^{n=m} {}^nL^{\phi}_{i,j}(x_i - x_j)^n \quad (4)$$

with ${}^nL^{\phi}_{i,j} = a_n + b_n \times T$ $(n = 0, 1 \ldots, m)$, where ${}^nL^{\phi}_{i,j}$ are the interaction parameters, $m + 1$ is the number of terms, and a_n and

Please cite this article in press as: S. Wasiur-Rahman, M. Medraj, A thermodynamic description of the Al–Ca–Zn ternary system, CALPHAD: Computer Coupling of Phase Diagrams and Thermochemistry (2009), doi:10.1016/j.calphad.2009.06.001

Table 4
Optimized model parameters of all the terminal solid solutions and stoichiometric compounds of the Al–Zn, Al–Ca and Ca–Zn systems.

Terminal solid solution			
Phase	Gibbs energy parameters (J/mol)		
Al_FCC	$\Delta^{ex}G^{Al_{FCC}}_{AlZn} = 3803.8 + 0.25T + (313.83 - 1.34T)X_{AlAl} + (-3347.34 - 0.418T)X_{ZnZn}$		
Zn_HCP	$G^{HCP}_{Al:Zn} = 13377.88 + 0.438T$		
Stoichiometric compounds			
Compound	$\Delta H^0_{298.15\ K}$ (J/mol-atom)	$\Delta S^0_{298.15\ K}$ (J/mol-atom. K)	C_p (J/mol K)
Al_4Ca	−18506.59	−3.31	$C_p = 4 \times C_p$(Al, FCC-A1) + C_p(Ca, BCC-A2)
Al_2Ca	−30225.80	−6.29	$C_p = 2 \times C_p$(Al, FCC-A1) + C_p(Ca, BCC-A2)
$Al_{14}Ca_{13}$	−25111.14	−5.14	$C_p = 14 \times C_p$(Al, FCC-A1) + $13 \times C_p$(Ca, BCC-A2)
Al_3Ca_8	−16254.45	−4.78	$C_p = 3 \times C_p$(Al, FCC-A1) + $8 \times C_p$(Ca, BCC-A2)
Ca_3Zn	−11906.31	−3.82	$C_p = 3 \times C_p$(Ca, BCC-A2) + C_p(Zn, HCP-Zn)
Ca_5Zn_3	−14486.92	−0.88	$C_p = 5 \times C_p$(Ca, BCC-A2) + $3 \times C_p$(Zn, HCP-Zn)
CaZn	−17842.54	−0.53	$C_p = C_p$(Ca, BCC-A2) + C_p(Zn, HCP-Zn)
$CaZn_2$	−22728.35	−1.48	$C_p = C_p$(Ca, BCC-A2) + $2 \times C_p$(Zn, HCP-Zn)
$CaZn_3$	−21418.76	−2.66	$C_p = C_p$(Ca, BCC-A2) + $3 \times C_p$(Zn, HCP-Zn)
$CaZn_5$	−19997.51	−3.84	$C_p = C_p$(Ca, BCC-A2) + $5 \times C_p$(Zn, HCP-Zn)
$CaZn_{11}$	−14798.75	−3.62	$C_p = C_p$(Ca, BCC-A2) + $11 \times C_p$(Zn, HCP-Zn)
$CaZn_{13}$	−14149.64	−4.23	$C_p = C_p$(Ca, BCC-A2) + $13 \times C_p$(Zn, HCP-Zn)

Table 5
Optimized model parameters for ternary solutions and compounds in the present study.

Liquid phase (J/mol)			
$L_{AlCa(Zn)} = -3854.0$, $L_{AlZn(Ca)} = -4100.0$, $L_{CaZn(Al)} = -35530.0$			
Stoichiometric compounds			
Compound	$\Delta H^0_{298.15\ K}$ (J/mol-atom)	$\Delta S^0_{298.15\ K}$ (J/mol-atom. K)	C_p (J/mol K)
CaAlZn	−33000.0	0.748	$C_p = C_p$(Ca, BCC-A2) + C_p(Al, FCC-A1) + C_p(Zn, HCP-Zn)
$CaAl_2Zn_2$	−29700.0	0.449	$C_p = C_p$(Ca, BCC-A2) + $2 \times C_p$(Al, FCC-A1) + $2 \times C_p$(Zn, HCP-Zn)

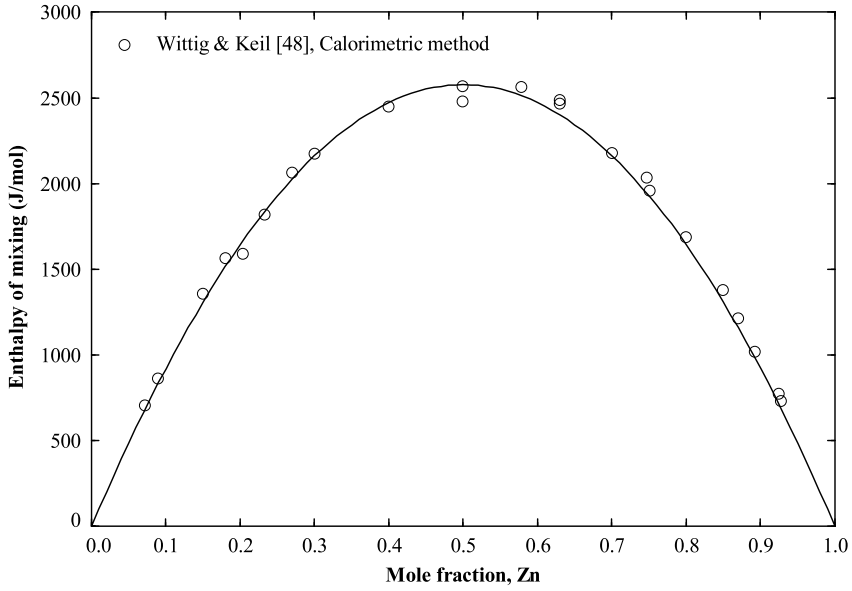

Fig. 2. Calculated enthalpies of mixing of Al and Zn in liquid Al–Zn alloy at 953 K in comparison with the experimental results (Reference state: Al_Liquid and Zn_Liquid).

b_n are the parameters of the model that need to be optimized considering the experimental phase diagram and thermodynamic data.

In the present work, one terminal solid solution phase, Zn_HCP of the Al–Zn system, was described using this model with one set of Redlich–Kister parameters.

The modified quasichemical model (MQM) in the pair approximation was selected to describe the liquid phases of the constituent binary systems. Alloy systems which show a strong compound forming tendency in the solid state also display a pronounced minimum in the enthalpy of mixing of the liquid phase and this is caused by the existence of short-range ordering [72]. The Bragg–Williams (BW) random-mixing model is not able to represent binary solutions with short-range ordering and to describe the enthalpy and entropy of mixing functions properly. The "associate" or "molecular" model [73] was also proposed in the literature to deal with the short-range ordering. However, the associate model assumes that some molecules occupy some of the atomic sites, which is not physically sound. Another important weakness of the "associate" model is its inability to predict the correct thermodynamic properties of ternary solutions when the binary subsystems exhibit short-range ordering [74]. The MQM has been

Please cite this article in press as: S. Wasiur-Rahman, M. Medraj, A thermodynamic description of the Al–Ca–Zn ternary system, CALPHAD: Computer Coupling of Phase Diagrams and Thermochemistry (2009), doi:10.1016/j.calphad.2009.06.001

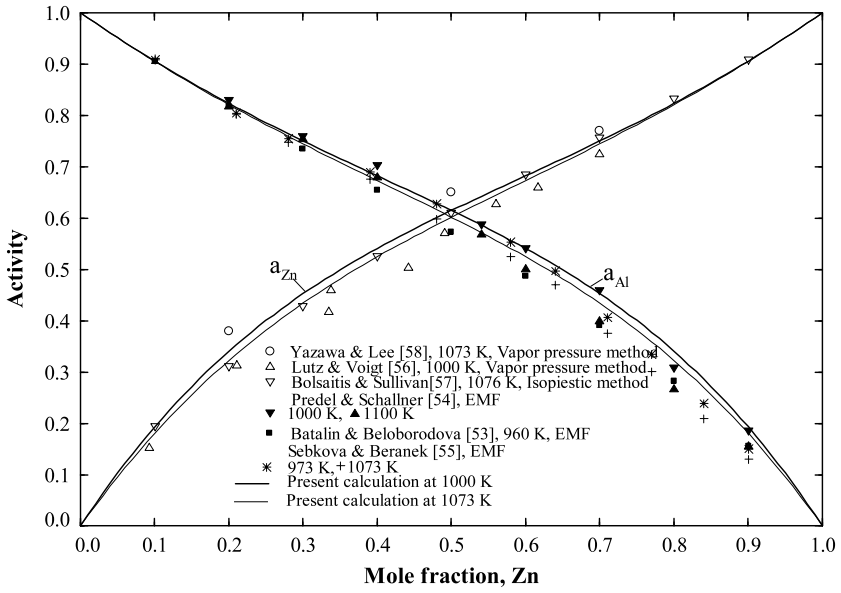

Fig. 3. Calculated activities of Al and Zn in the liquid state at 1000 K and 1073 K (Reference state: Al_Liquid and Zn_Liquid).

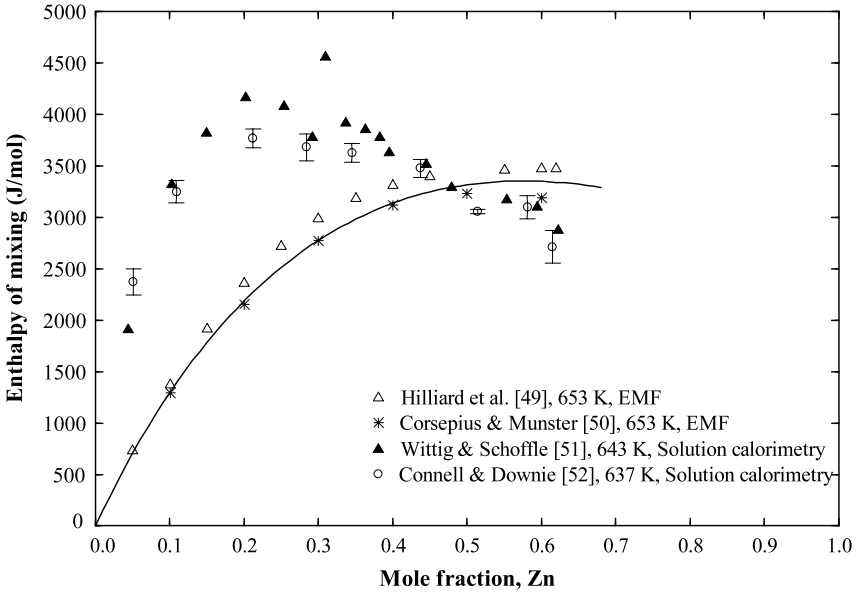

Fig. 4. Calculated enthalpies of mixing in the Al_FCC solid solution at 653 K in comparison with the experimental results (Reference state: Al_FCC and Zn_HCP).

described extensively elsewhere [75–77], and will be outlined briefly here. In the pair approximation of the MQM, the simple pair exchange reaction between atoms A and B on neighboring lattice sites is considered as follows:

$$(A\text{–}A)_{pair} + (B\text{–}B)_{pair} = 2(A\text{–}B)_{pair};\ \Delta g_{AB} \tag{5}$$

where $(A\text{–}B)$ represents a first-nearest-neighbor pair and Δg_{AB} is the nonconfigurational Gibbs energy change for the formation of two moles of $(A\text{–}B)$ pairs. According to Pelton et al. [75–77], the molar Gibbs energy of a binary A–B solution is given as

$$G^{liq} = \left(n_A{}^0g_A^{liq} + n_B{}^0g_B^{liq}\right) - T\Delta S^{config} + \left(\frac{n_{AB}}{2}\right)\Delta g_{AB}. \tag{6}$$

Here n_A and n_B are the number of moles of component A and B, n_{AB} is the number of moles of $(A\text{–}B)$ pairs, and ΔS^{config} is the configurational entropy of mixing given by a random distribution of the $(A-A)$, $(B-B)$ and $(A\text{–}B)$ pairs. Pelton et al. [75] made a modification to Eq. (6) by expanding Δg_{AB} as a polynomial in terms of the pair fraction X_{AA} and X_{BB} as shown in Eq. (7):

$$\Delta g_{AB} = \Delta g^o_{AB} + \sum_{i\geq 1} g^{i0}_{AB}X^i_{AA} + \sum_{j\geq 1} g^{0j}_{AB}X^j_{BB} \tag{7}$$

where Δg^o_{AB}, g^{i0}_{AB} and g^{0j}_{AB} are the model parameters to be optimized; they can be expressed as functions of temperature ($\Delta g^o_{AB} = a + bT$). In addition, a further modification has been made in the coordination numbers by making them composition-dependent in order to overcome the drawbacks of the constant coordination numbers. This modification can be expressed as

$$\frac{1}{Z_A} = \frac{1}{Z^A_{AA}}\left(\frac{2n_{AA}}{2n_{AA}+n_{AB}}\right) + \frac{1}{Z^A_{AB}}\left(\frac{n_{AB}}{2n_{AA}+n_{AB}}\right) \tag{8}$$

$$\frac{1}{Z_B} = \frac{1}{Z^B_{BB}}\left(\frac{2n_{BB}}{2n_{BB}+n_{AB}}\right) + \frac{1}{Z^B_{BA}}\left(\frac{n_{AB}}{2n_{BB}+n_{AB}}\right) \tag{9}$$

where Z^A_{AA} and Z^A_{AB} are the values of Z_A when all nearest neighbors of an A atom are A's, and when all nearest neighbors of an A atom

Please cite this article in press as: S. Wasiur-Rahman, M. Medraj, A thermodynamic description of the Al–Ca–Zn ternary system, CALPHAD: Computer Coupling of Phase Diagrams and Thermochemistry (2009), doi:10.1016/j.calphad.2009.06.001

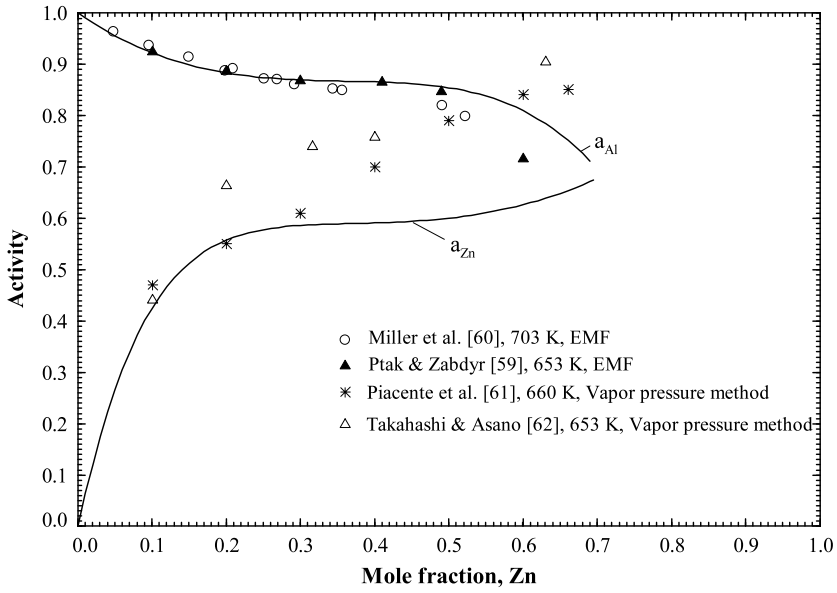

Fig. 5. Calculated activities of Al and Zn in the Al_FCC phase at 653 K (Reference state: Al_FCC and Zn_HCP).

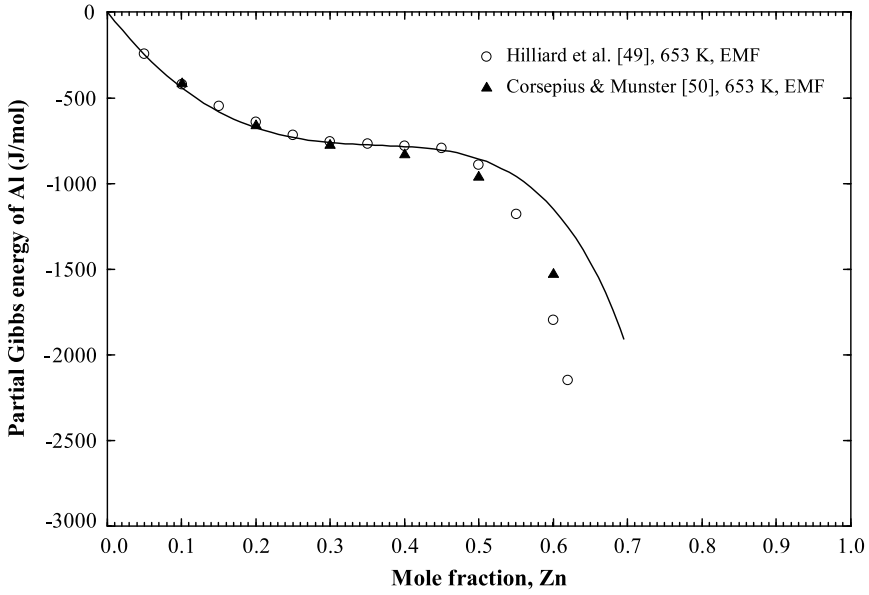

Fig. 6. Calculated partial Gibbs energy of Al in the Al_FCC phase at 653 K (Reference state: Al_FCC and Zn_HCP).

are B's, respectively. Similarly for Z^B_{BB} and Z^B_{BA}. The composition of maximum short-range ordering is determined by the ratio $\frac{Z^B_{BA}}{Z^A_{AB}}$. Values of Z^A_{AB} and Z^B_{BA} are unique to the A–B binary system and should be carefully determined to fit the thermodynamic experimental data (enthalpy of mixing, activity etc.). In the case of a solid solution (i.e. Al_FCC phase in the Al–Zn system), it is required that $Z^A_{AA} = Z^B_{BB} = Z^A_{AB} = Z^B_{BA}$ due to their rigid lattice structure. The values of Z^A_{AA} and Z^B_{BB} are common for all systems containing A and B as components. The coordination number of the pure elements in the metallic solution, $Z^{Al}_{AlAl} = Z^{Ca}_{CaCa} = Z^{Zn}_{ZnZn}$, was set to be 6, because this value gave the best possible fit for many binary systems and was also recommended by Pelton et al. [75–77]. For the liquid phase, the values of Z^{Al}_{AlZn}, Z^{Zn}_{ZnAl}, Z^{Ca}_{CaZn}, Z^{Zn}_{ZnCa}, Z^{Al}_{AlCa} and Z^{Ca}_{CaAl} are chosen to permit the composition of maximum short-range ordering in the binary system to be consistent with the composition that corresponds to the minimum enthalpy of mixing. These values are listed in Table 2.

All the optimized model parameters of different phases in the Al–Ca–Zn ternary system are summarized in Tables 2, 4 and 5.

4. Results and discussions

4.1. Al–Zn binary system

The calculated Al–Zn binary system is shown in Fig. 1, which shows reasonable agreement with the experimental data from the literature. The isobaric phase diagram shows a large FCC solid solution with a miscibility gap and Zn-rich HCP solid solution. Apart from a few discrepancies for the miscibility gap in the FCC phase, the phase diagram shows reasonable agreement with all the experimental points. As shown in Fig. 1, the model calculated miscibility gap for the Al-rich portion is high in temperature. However, there are appreciable disagreements between the experimental data obtained by different groups of investigators for the FCC miscibility gap as well as for the Al_FCC$_2$/(Al_FCC+Zn_HCP) phase

Please cite this article in press as: S. Wasiur-Rahman, M. Medraj, A thermodynamic description of the Al–Ca–Zn ternary system, CALPHAD: Computer Coupling of Phase Diagrams and Thermochemistry (2009), doi:10.1016/j.calphad.2009.06.001

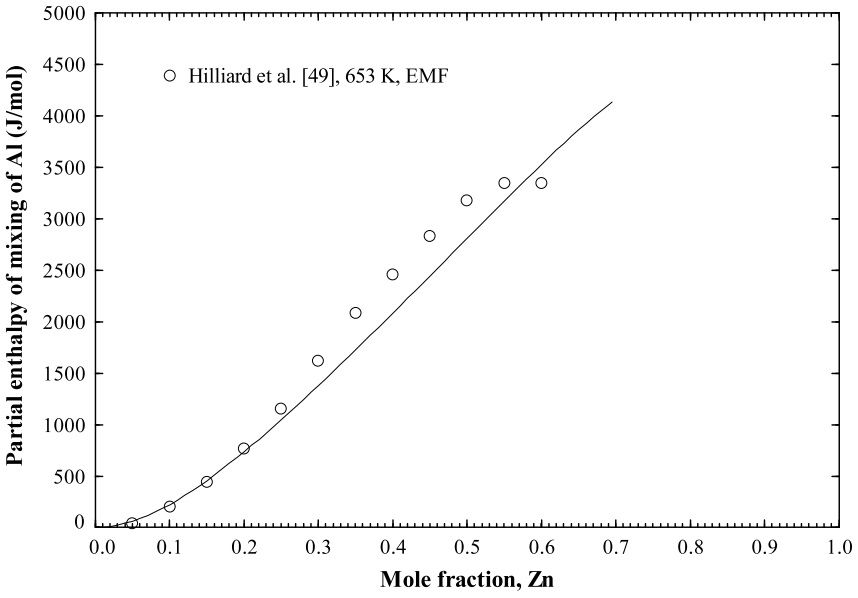

Fig. 7. Calculated partial enthalpy of mixing of Al in the Al_FCC phase at 653 K (Reference state: Al_FCC and Zn_HCP).

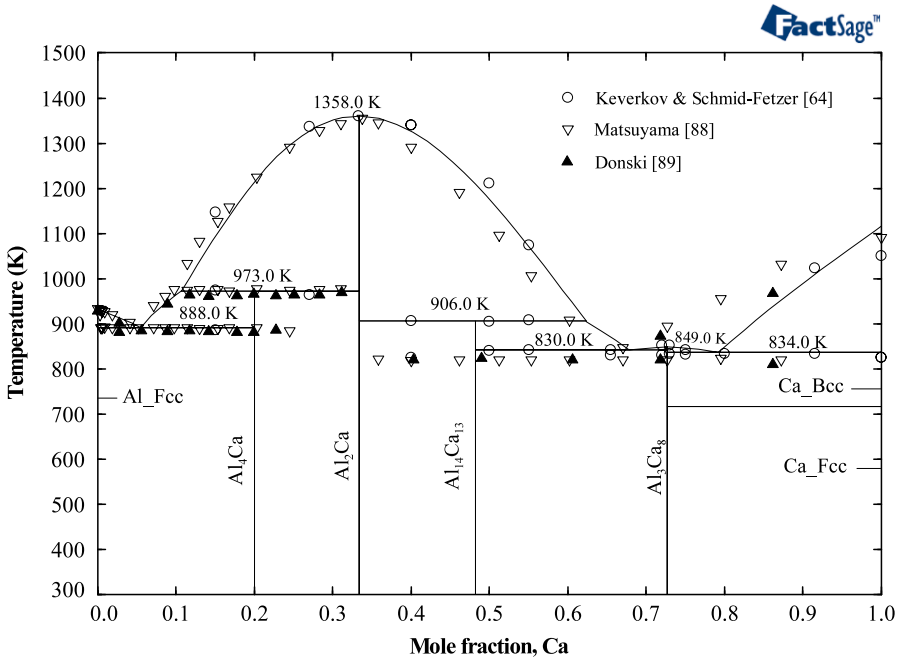

Fig. 8. Re-optimized Al–Ca phase diagram in comparison with the experimental results from the literature [64,88,89].

boundary, and the current calculation generally falls within the experimental data. Better agreement in this composition range was not possible without deteriorating the consistency with the thermodynamic properties. A similar difficulty was encountered by other researchers [11–15] during the previous efforts to model this system. Their calculated phase diagram showed significant discrepancy with the experimental results especially in the FCC miscibility gap and in the Al_FCC/(Al_FCC+Liquid) phase boundary. The solubility of Zn in Al increases from 0.33 at.% Zn at room temperature to 16.0 at.% Zn at the eutectoid temperature, which is 555 K. Above this temperature, the solvus curve lies on the Zn-rich side of the FCC miscibility gap where the solubility increases from 58.4 at.% Zn at 555 K to 68.0 at.% Zn at the eutectic temperature of 651 K. The maximum solubility of Al in Zn was found to be 2.8 at.% Al at the eutectic temperature, which lies between the 2.6 and 2.9 at.% Al values reported by Auer and Mann [42] and Lohberg [45], respectively. Table 3 lists all the invariant points calculated in the present work in comparison with the experimental results.

It is important to note that Rudman and Averbach [78] observed evidence of short-range ordering in the Al_FCC solid solution during their experiments on this system. Hence, the modified quasichemical model has been employed for the Al_FCC substitutional solid solution and for the liquid phase in this work. For the Zn_HCP solid solution, the Bragg–Williams model represented by the Redlich–Kister polynomial [63] is used.

The calculated enthalpy of mixing of the liquid phase in the Al–Zn system at 953 K is shown in Fig. 2. Good agreement has been achieved between the calculated results and the calorimetric data of Wittig and Keil [48]. The endothermic trend of the enthalpy of mixing is obvious due to the flat nature of the liquidus curve in

Please cite this article in press as: S. Wasiur-Rahman, M. Medraj, A thermodynamic description of the Al–Ca–Zn ternary system, CALPHAD: Computer Coupling of Phase Diagrams and Thermochemistry (2009), doi:10.1016/j.calphad.2009.06.001

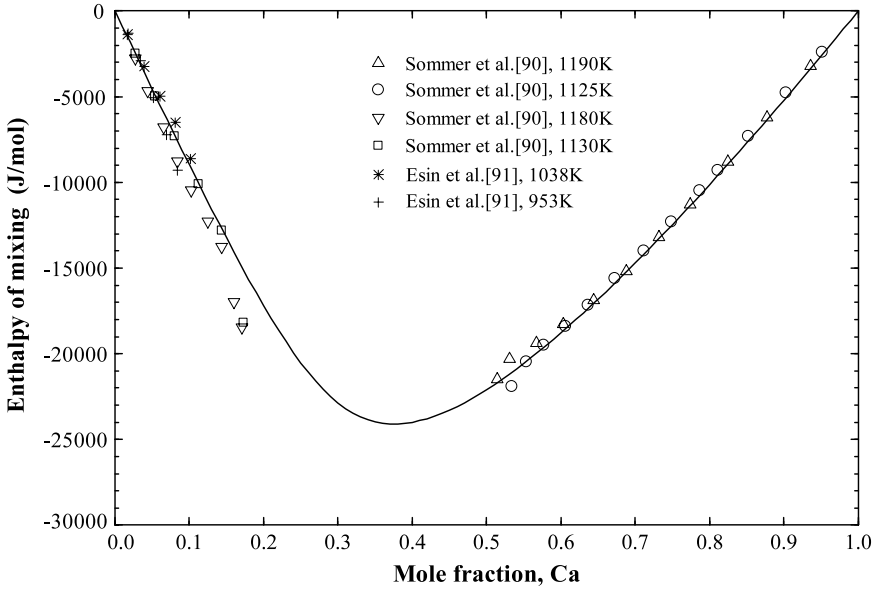

Fig. 9. Calculated enthalpies of mixing of Al and Ca in liquid Al–Ca alloy at 1100 K in comparison with the experimental results (Reference state: Al_Liquid and Ca_Liquid). Experimental points are from [90,91].

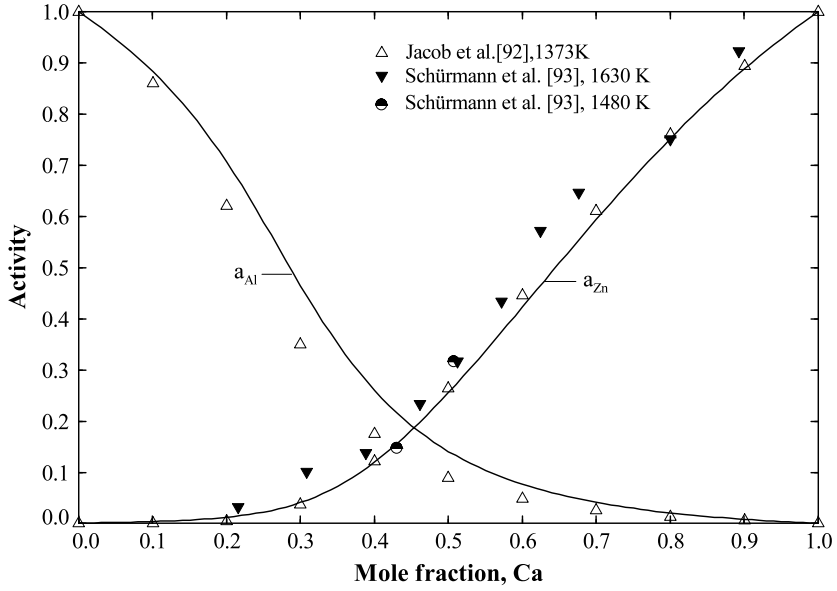

Fig. 10. Calculated activities of Al and Ca in the liquid state at 1373 K (Reference state: Al_Liquid and Ca_Liquid). Experimental points are from [92,93].

the phase equilibrium diagram. It also reflects the fact that the formation of Al–Al and Zn–Zn pairs is more favorable than the formation of Al–Zn pairs in the liquid phase. The calculated activity in the liquid Al–Zn alloys at 1000 K and 1073 K can be seen in Fig. 3. As expected, the activities of both Al and Zn show positive deviation from the ideal solution behavior. It can be seen from the same figure that the activity of Zn at different temperatures shows some deviation from the results of Lutz and Voigt [56] and Yazawa and Lee [58] but agrees well with the values of Bolsaitis and Sullivan [57]. This is due to the less accurate vapor pressure method used by Lutz and Voigt [56] and Yazawa and Lee [58].

Fig. 4 illustrates the calculated enthalpy of mixing in the extended Al_FCC solid solution at 653 K in comparison with the experimental results from the literature. Reasonable consistency has been achieved with the EMF results of Hilliard et al. [49] and Corsepius and Munster [50] but the current calculation differs markedly from the solution calorimetric results of Wittig and Schoffl [51] and Connell and Downie [52]. These results [51,52] show that in the composition region around 50.0 at.% Zn there is a fall in the enthalpy values, which indicates an ordered phase formation in the solid solution, though no confirmatory evidence of it could be found. The most reliable experimental works of Gayler et al. [24], Morinaga [30], Ellwood [32] and Fink and Willey [34] on the phase equilibrium diagram also could not find evidence of any kind of phase change, and hence more emphasis has been given to the results of Hilliard et al. [49] and Corsepius and Munster [50] in the present assessment.

The calculated activity of Al and Zn and the partial Gibbs energy of Al in the FCC phase at 653 K are shown in Figs. 5 and 6, respectively. The Al activity curve shows good consistency with the experimental points whereas the activity of Zn shows a large deviation from the experimental points in Fig. 5. This temperature (653 K) is only about 25 K higher than the critical temperature of the miscibility gap. Due to the close proximity

Please cite this article in press as: S. Wasiur-Rahman, M. Medraj, A thermodynamic description of the Al–Ca–Zn ternary system, CALPHAD: Computer Coupling of Phase Diagrams and Thermochemistry (2009), doi:10.1016/j.calphad.2009.06.001

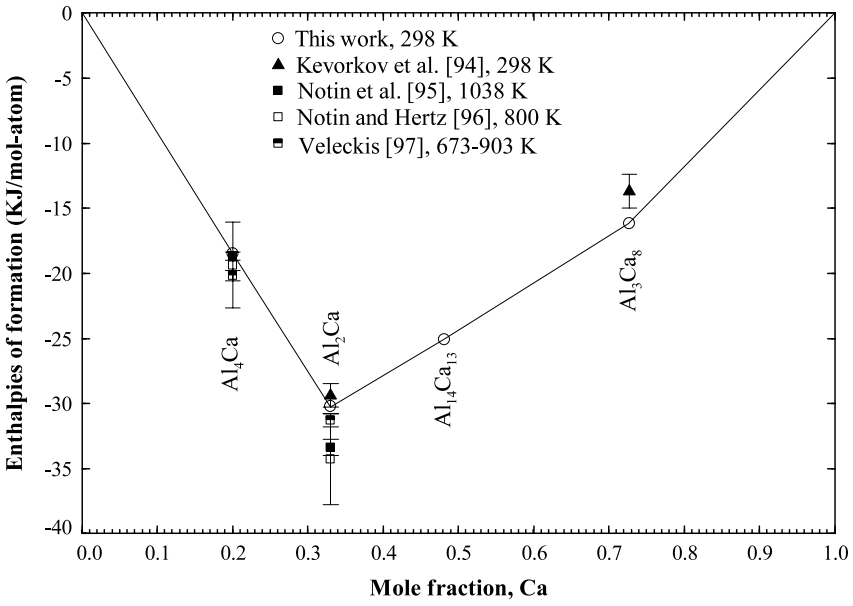

Fig. 11. Re-optimized enthalpies of formation at 298 K for the compounds in the Al–Ca system (Reference state: Al_FCC and Ca_BCC). Experimental points are from [94–97].

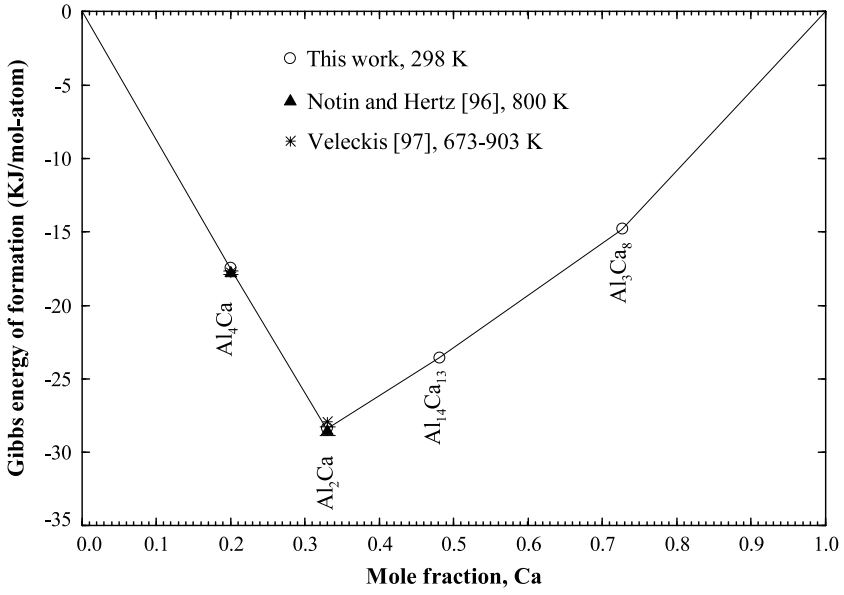

Fig. 12. Re-optimized Gibbs energies of formation at 298 K for the compounds in the Al–Ca system (Reference state: Al_FCC and Ca_BCC).

of this temperature to the miscibility gap, the behavior of the thermodynamic properties can be expected to be similar to that of the miscibility gap. Hence at 653 K, the Gibbs energy curve is expected to be flat enough, similar to the miscibility gap in the composition range of 25.0 to 45.0 at.% Zn. This means that the partial Gibbs energy will change slowly with increasing composition, as shown in Fig. 6. However, the values obtained by Piacente et al. [61] and Takahashi and Asano [62] change rapidly with composition; both of them used the vapor pressure method, which is less accurate than the EMF method used by Ptak and Zabdyr [59] and Miller et al. [60]. Nevertheless, the current assessment is consistent with the experimental results for the Al activity, partial Gibbs energy and partial enthalpy of mixing, as can be seen in Figs. 5–7.

The calculated partial Gibbs energy of Al in the FCC phase can be seen in Fig. 6, where reasonable agreement with the experimental data of Hilliard et al. [49] and Corsepius and Munster [50] was obtained except for some mismatch at higher than 50.0 at.% Zn. Fig. 7 shows the calculated partial enthalpy of mixing of Al at 653 K in comparison with the experimental points of Hilliard et al. [49], where good agreement is accomplished.

4.2. Al–Ca binary system

The most recent work on the Al–Ca binary system has been carried out by Aljarrah and Medraj [16]. They also used the modified quasichemical model to describe the liquid phase. In the present work, some modifications have been made by adjusting the values of the composition-dependent coordination numbers and the excess Gibbs energy parameters to increase the consistency with the experimental results.

The re-optimized Al–Ca binary system is shown in Fig. 8, which shows reasonable agreement with the experimental data from the literature. Table 6 lists all the invariant points in comparison with

Please cite this article in press as: S. Wasiur-Rahman, M. Medraj, A thermodynamic description of the Al–Ca–Zn ternary system, CALPHAD: Computer Coupling of Phase Diagrams and Thermochemistry (2009), doi:10.1016/j.calphad.2009.06.001

Table 6
Comparison between the present calculation and the calculated and experimental values from the literature of the invariant reactions in the Al–Ca system.

Reaction type	Reaction	Composition (at.% Ca)	Temperature (K)	Reference
Eutectic	$L \leftrightarrow Al\_FCC + Al_4Ca$	5.5	888.0	This work
		4.8	885.2	[16]
		5.1	886.2	[64]
		5.2	889.2	[89]
		5.5	883.2	[90]
	$L \leftrightarrow Al_{14}Ca_{13} + Al_3Ca_8$	67.8	830.0	This work
		66.5	830.2	[16]
		66.3	829.2	[64]
		64.5	818.2	[89]
		66.9	823.2	[90]
	$L \leftrightarrow Ca\_BCC + Al_3Ca_8$	79.3	834.0	This work
		79.6	827.2	[16]
		80.0	833.2	[64]
Peritectic	$L + Al_2Ca \leftrightarrow Al_4Ca$	10.5	973.0	This work
		8.0	973.2	[16]
		–	973.2	[64]
		–	973.2	[89]
		–	963.2	[90]
	$L + Al_2Ca \leftrightarrow Al_{14}Ca_{13}$	62.2	906.0	This work
		61.0	904.2	[16]
		–	906.2	[64]
Congruent	$L \leftrightarrow Al_2Ca$	33.3	1358.0	This work
		33.3	1356.2	[16]
		33.3	1359.2	[64]
		33.3	1352.2	[89]
	$L \leftrightarrow Al_3Ca_8$	72.7	849.0	This work
		72.7	843.2	[16]
		72.7	852.2	[64]

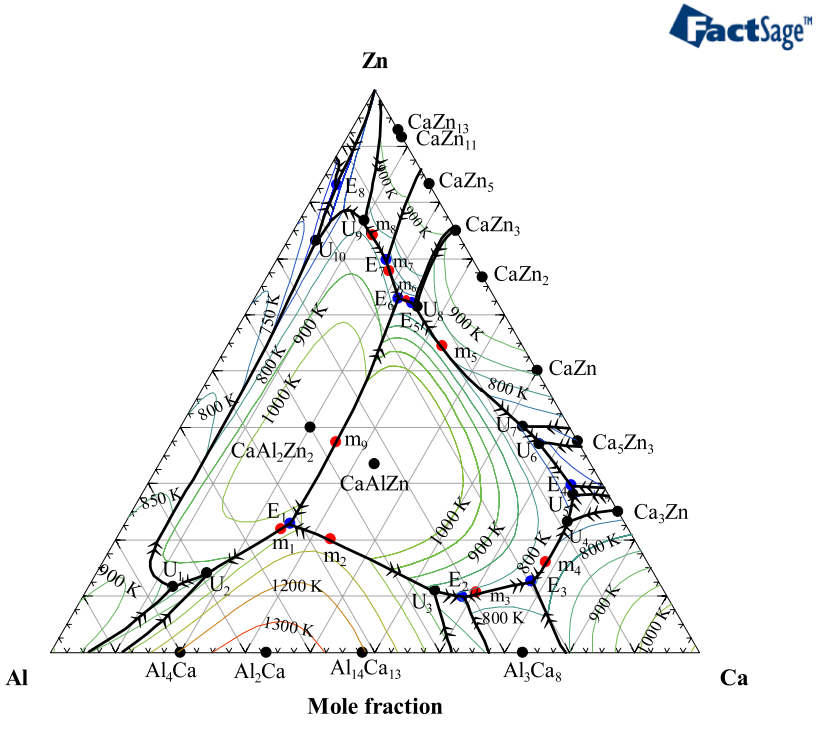

Fig. 13. Calculated liquidus surface of the Al–Ca–Zn ternary system.

the experimental data as well as the calculation of Aljarrah and Medraj [16].

The re-optimized excess Gibbs energy parameters have also been used to calculate the different thermodynamic properties in the liquid and solid phases of the Al–Ca system. Figs. 9 and 10 depict the calculated enthalpy of mixing and activities of Al and Ca in the liquid phase along with the experimental values from the literature. Reasonable agreement with the experimental results can be seen from these figures, apart from some discrepancy for the activity of Al. Better agreement was not possible without deteriorating the liquidus curve. Figs. 11 and 12 illustrate the calculated enthalpies of formation and the Gibbs energies of formation for the stoichiometric compounds in comparison with the available experimental results. The calculated and the measured values are in good accord with each other, as can be seen from those figures.

Please cite this article in press as: S. Wasiur-Rahman, M. Medraj, A thermodynamic description of the Al–Ca–Zn ternary system, CALPHAD: Computer Coupling of Phase Diagrams and Thermochemistry (2009), doi:10.1016/j.calphad.2009.06.001

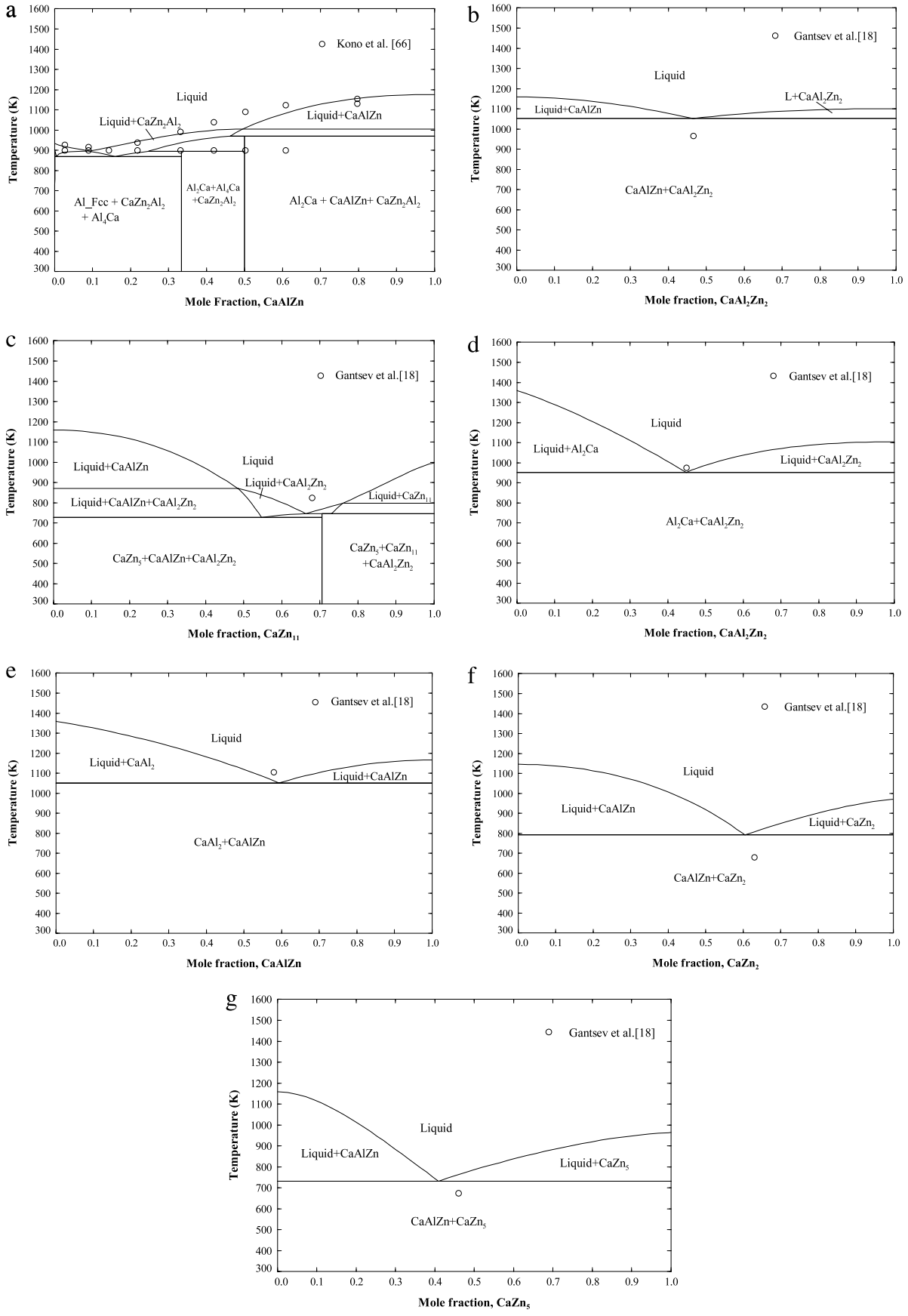

Fig. 14. Calculated isoplethal analysis of sections (a) Al–CaAlZn, (b) CaAlZn–$CaAl_2Zn_2$, (c) CaAlZn–$CaZn_{11}$, (d) Al_2Ca–$CaAl_2Zn_2$, (e) Al_2Ca–CaAlZn, (f) CaAlZn–$CaZn_2$, (g) CaAlZn–$CaZn_5$.

Please cite this article in press as: S. Wasiur-Rahman, M. Medraj, A thermodynamic description of the Al–Ca–Zn ternary system, CALPHAD: Computer Coupling of Phase Diagrams and Thermochemistry (2009), doi:10.1016/j.calphad.2009.06.001

Table 7
Calculated four-phase equilibria points and their reactions in the Al–Ca–Zn system.

Type	Reaction	Composition (at.%)			Temp (K)	Reference
		Al	Zn	Ca		
E_1	$L \leftrightarrow Al_2Ca + CaAlZn + CaAl_2Zn_2$	51.8	22.7	25.8	952.0	This work
E_2	$L \leftrightarrow Al_{14}Ca_{13} + Al_3Ca_8 + CaAlZn$	31.5	9.6	58.9	777.2	This work
E_3	$L \leftrightarrow Ca\_BCC + Al_3Ca_8 + CaAlZn$	19.6	12.4	68.0	752.2	This work
E_4	$L \leftrightarrow CaAlZn + Ca_3Zn + Ca_5Zn_3$	4.8	29.5	65.7	648.0	This work
E_5	$L \leftrightarrow CaZn_5 + CaAlZn + CaZn_3$	12.9	61.9	25.2	729.9	This work
E_6	$L \leftrightarrow CaAlZn + CaZn_5 + CaAl_2Zn_2$	14.8	62.9	22.3	729.5	This work
E_7	$L \leftrightarrow CaZn_5 + CaZn_{11} + CaAl_2Zn_2$	13.4	69.6	17.0	748.8	This work
E_8	$L \leftrightarrow Zn\_HCP + Al\_FCC + CaZn_{13}$	13.6	84.0	2.4	636.4	This work
		11.18	88.46	0.46	653.0	[66]
U_1	$L + Al_4Ca \leftrightarrow Al\_FCC + CaAl_2Zn_2$	75.3	11.6	13.1	818.0	This work
U_2	$L + Al_2Ca \leftrightarrow Al_4Ca + CaAl_2Zn_2$	69.0	14.0	17.0	848.3	This work
U_3	$L + Al_2Ca \leftrightarrow Al_{14}Ca_{13} + CaAlZn$	35.6	10.6	53.8	823.7	This work
U_4	$L + Ca\_BCC \leftrightarrow CaAlZn + Ca\_FCC$	8.5	23.2	68.3	716.0	This work
U_5	$L + Ca\_FCC \leftrightarrow CaAlZn + Ca_3Zn$	8.9	29.6	61.5	630.0	This work
U_6	$L + CaZn \leftrightarrow CaAlZn + Ca_5Zn_3$	6.2	37.2	56.6	662.2	This work
U_7	$L + CaZn_2 \leftrightarrow CaZn + CaAlZn$	7.0	40.2	52.8	678.0	This work
U_8	$L + CaZn_2 \leftrightarrow CaZn_3 + CaAlZn$	12.7	61.5	25.8	732.0	This work
U_9	$L + CaZn_{11} \leftrightarrow CaAl_2Zn_2 + CaZn_{13}$	13.4	76.5	10.1	767.0	This work
U_{10}	$L + CaAl_2Zn_2 \leftrightarrow Al\_FCC + CaZn_{13}$	21.6	73.5	4.9	620.0	This work
m_1	$L \leftrightarrow Al_2Ca + CaAl_2Zn_2$	53.0	22.0	25.0	962.0	This work
		48.8	24.8	26.4	983.0	[18]
m_2	$L \leftrightarrow Al_2Ca + CaAlZn$	18.0	50.0	32.0	1080.0	This work
		15.2	51.5	33.3	1123.0	[18]
m_3	$L \leftrightarrow Al_3Ca_8 + CaAlZn$	29.0	10.6	60.4	779.0	This work
m_4	$L \leftrightarrow CaAlZn + Ca\_BCC$	15.7	16.0	68.3	760.3	This work
m_5	$L \leftrightarrow CaAlZn + CaZn_2$	9.9	57.0	33.1	786.0	This work
		7.6	59.1	33.3	648.0	[18]
m_6	$L \leftrightarrow CaAlZn + CaZn_5$	13.8	62.8	23.4	710.0	This work
		–	–	–	653.0	[18]
m_7	$L \leftrightarrow CaAl_2Zn_2 + CaZn_5$	13.8	67.9	18.3	748.5	This work
m_8	$L \leftrightarrow CaZn_{11} + CaAl_2Zn_2$	13.3	74.1	12.5	775.5	This work
m_9	$L \leftrightarrow CaAlZn + CaAl_2Zn_2$	37.0	37.0	26.0	1013.0	This work
		36.4	36.4	27.2	923.0	[18]

4.3. Al–Ca–Zn ternary system

A self-consistent thermodynamic database for the Al–Ca–Zn system has been created by extrapolating the three constituting binaries. Ternary interaction parameters were used in order to achieve consistency with the available experimental data from the literature. The asymmetric Toop geometric model [79] was used for the extrapolation since Al and Ca are chemically similar but different from Zn. Two ternary compounds, CaAlZn and $CaAl_2Zn_2$, reported by Ganiev et al. [17] and Gantsev et al. [18] were considered during the present optimization.

The liquidus projection of the Al–Ca–Zn system is shown in Fig. 13, where the heavier solid lines represent the univariant valleys and the arrows on these lines indicate the directions of decreasing temperature. There are eight ternary eutectic (E_1 to E_8) points, ten quasi-peritectic (U_1 to U_{10}) points and nine maximum (m_1 to m_9) points present in this system. Details of all the ternary invariant points are summarized in Table 7.

4.3.1. Isoplethal analysis

Both Kono et al. [66] and Gantsev et al. [18] reported some pseudo-binary sections which will be compared with the present calculation. Fig. 14 compares the current work with all the vertical sections reported by the different experimental works of Kono et al. [66] and Gantsev et al. [18]. From Fig. 14, it can be seen that most of the pseudo-binary sections show reasonable agreement with the experimental results. However, it was impossible to obtain complete consistency with the two different sets of experiments because they assumed different ternary compounds. Due to this fact, the sub-liquidus phases can sometimes be different from the experimental results, as can be seen in Fig. 14(a).

From Fig. 14(b) to Fig. 14(g) some discrepancy can be observed with the experimental points of Gantsev et al. [18], where they only reported the saddle point for each pseudo-binary section. More experimental work on the liquidus curve is necessary for adequate validation in this regard.

5. Concluding remarks

Gibbs energy functions for all phases in the Al–Ca–Zn system have been obtained through the establishment of a comprehensive database for this system. All the available thermodynamic and phase equilibrium data have been critically evaluated in order to obtain one set of optimized model parameters of the Gibbs energies for all the phases. The optimized binary phase diagrams as well as the different thermodynamic properties such as integral enthalpy of mixing, enthalpy of formation of the compounds and partial properties such as activity and partial enthalpy of mixing show reasonable agreement with the available experimental data. The modified quasichemical model has been used for the liquid phase and Al_FCC phase of the Al–Zn system in order to account for the presence of short-range ordering. The consideration of the two ternary compounds reported by most of the researchers resulted in a reasonable agreement with the experimental results from the literature. Nevertheless, additional experimental work is necessary to obtain more information about the ternary compounds (CaAlZn and $CaAl_2Zn_2$) regarding their melting points, crystal structure, solubility limits and enthalpies of formation. The present work can act as a guideline for conducting key experiments in this regard.

Acknowledgments

Financial support from the Natural Sciences and Engineering Research Council of Canada (NSERC) is gratefully acknowledged.

Please cite this article in press as: S. Wasiur-Rahman, M. Medraj, A thermodynamic description of the Al–Ca–Zn ternary system, CALPHAD: Computer Coupling of Phase Diagrams and Thermochemistry (2009), doi:10.1016/j.calphad.2009.06.001

Appendix. Supplementary data

Supplementary data associated with this article can be found, in the online version, at doi:10.1016/j.calphad.2009.06.001.

References

[1] T.G. Nieh, J. Wadsworth, Superplasticity and superplastic forming of aluminum metal matrix composites, Journal of Metals 44 (11) (1992) 46–50.
[2] V.A. Shvets, V.O. Lavrenko, V.M. Talash, Experience of application of protectors made of Al–Zn–Ca alloys, Materials Science 42 (4) (2006) 563–565.
[3] D.M. Moore, L.R. Morris, US patent 4, 126, 448, November, 1978.
[4] M. Aljarrah, Thermodynamic modeling and experimental investigation of the Mg–Al–Ca–Sr system, Ph.D. Thesis, Concordia University, Montreal, Canada, 2008.
[5] P. Liang, T. Tarfa, J.A. Robinson, S. Wagner, P. Ochin, M.G. Harmelin, H.J. Seifert, H.L. Lukas, F. Aldinger, Experimental investigation and thermodynamic calculation of the Al–Mg–Zn system, Thermochemica Acta 314 (1998) 87–110.
[6] Y.B. Kim, F. Sommer, B. Predel, Calorimetric investigation of liquid aluminum–magnesium–zinc alloys, Journal of Alloys and Compounds 247 (1997) 43–51.
[7] M. Ohno, D. Mirkovic, R. Schmid-Fetzer, Phase equilibria and solidification of Mg-rich Mg–Al–Zn Alloys, Materials Science & Engineering, A: Structural Materials: Properties, Microstructure and Processing A421 (1–2) (2006) 328–337.
[8] P. Donnadieu, A. Quivy, T. Tarfa, P. Ochin, A. Dezellus, M.G. Harmelin, P. Liang, H.L. Lukas, H.J. Seifert, F. Aldinger, G. Effenberg, On the crystal structure and solubility range of the ternary phase in the Mg–Al–Zn system, Zeitschrift fuer Metallkunde 88 (12) (1997) 911–916.
[9] S. Wasiur-Rahman, M. Medraj, Critical assessment and thermodynamic modeling of the binary Mg–Zn, Ca–Zn and ternary Mg–Ca–Zn systems, Intermetallics 17 (10) (2009) 847–864.
[10] L. Kaufman, H. Bernstein, Computer Calculation of Phase Diagrams with Special Reference to Refractory Metals, Academic Press, New York, 1970.
[11] J.L. Murray, The aluminum–zinc system, Bulletin of Alloy Phase Diagrams 4 (1) (1983) 55–73.
[12] S.A. Mey, G. Effenberg, A thermodynamic evaluation of the aluminum–zinc system, Zeitschrift fur Metallkunde 77 (7) (1986) 449–453.
[13] S.A. Mey, Re-evaluation of the aluminum–zinc system, Zeitschrift fur Metallkunde 84 (7) (1993) 451–455.
[14] S.L. Chen, Y.A. Chang, A thermodynamic analysis of the Al–Zn system and phase diagram calculation, CALPHAD 17 (2) (1993) 113–124.
[15] M. Mathon, K. Jardet, E. Aragon, P. Satre, A. Sebaoun, Al–Ga–Zn system: Re-assessments of the three binary systems and discussion on possible estimations and on optimisation of the ternary system, CALPHAD 24 (3) (2000) 253–284.
[16] M. Aljarrah, M. Medraj, Thermodynamic assessment of the phase equilibria in the Al–Ca–Sr system using the modified quasichemical model, Journal of Chemical Thermodynamics 40 (4) (2008) 724–734.
[17] I.N. Ganiev, M.S. Shukroev, Kh.M. Nazarov, Effect of phase composition on the electrochemical behavior of aluminum–zinc–calcium alloys, Zhurnal Prikladnoi Khimii 68 (10) (1995) 1646–1649.
[18] I.N. Gantsev, K.M. Nazarov, M.M. Khakdodov, N.I. Gantseva, Interaction of binary eutectics in Al–Zn–Ca (Sr, Ba) systems, Evtektika V, Mizhnarodna Konferentsiya, Dnepropetrovsk, National Metallurgical Academy of Ukraine, Dnepropetrovsk, Ukraine, 2000, pp. 56–58.
[19] C. Bale, A.D. Pelton, W. Thompson, Factsage Thermochemical Software and Databases, 2008. http://www.crct.polymtl.ca.
[20] K.C. Kumar, P. Wollants, Some guidelines for thermodynamic optimization of phase diagrams, Journal of Alloys and Compounds 320 (2001) 189–198.
[21] C.T. Heycock, F.H. Neville, The freezing points of alloys containing zinc and another metal, Journal of the Chemical Society Transactions 71 (1897) 383–398.
[22] T. Tanabe, Studies in the aluminium–zinc system, Journal of the Institute of Metals 32 (1924) 415–427.
[23] T. Isihara, On the equilibrium diagram of the aluminum–zinc system, Science Reports of the Tohoku Imperial University 13 (1924) 18–21.
[24] M.L.V. Gayler, M. Haughton, E.G. Sutherland, The constitution of aluminum–zinc alloys of high purity: The nature of the thermal change of 443 °C, Journal of the Institute of Metals 63 (1938) 123–147.
[25] E. Pelzel, H. Schneider, Contribution to the understanding of Zn alloys, Zeitschrift fur Metallkunde 35 (1943) 124–127.
[26] E. Butchers, W. Hume-Rothery, On the constitution of aluminum–magnesium–manganese–zinc alloys: The solidus, Journal of the Institute of Metals 71 (1945) 291–311.
[27] E. Pelzel, The positions of the liquidus and solidus curves in the Al–Zn system from 30 to 70 wt.% Al, Zeitschrift fur Metallkunde 40 (1949) 134–136.
[28] I.S. Solet, H.W.S. Clair, Liquidus temperatures and liquid densities of zinc–aluminum alloys, Bureau of Mines Report of Investigations 4553 (1949) 1–7.
[29] Q.F. Peng, F.S. Chen, B.S. Qi, Y.S. Wang, Measurement of aluminum–zinc phase diagram by acoustic emission during solidification, Transactions of the American Foundrymen's Society 99 (1991) 199–202.
[30] T. Morinaga, On the equilibrium diagram of the aluminum–zinc system, Nippon Kinzoku Gakkaishi 3 (1939) 216–221.
[31] E. Gebhardt, Equilibrium experiments on the systems zinc–aluminum and zinc–aluminum–copper, Zeitschrift fur Metallkunde 40 (1949) 136–140.
[32] E.C. Ellwood, The solid solutions of zinc in aluminum, Journal of the Institute of Metals 80 (1951) 217–224.
[33] H. Araki, Y. Minamino, T. Yamane, K. Azuma, Y.S Kang, Y Miyamoto, Partial phase diagrams of the aluminum-rich region of the aluminum–zinc system at 0.1 MPa and 2.1 GPa, Journal of Materials Science Letters 11 (3) (1992) 181–183.
[34] W.L Fink, L.A. Willey, Equilibrium relations in aluminum–zinc alloys of high purity, II, Transactions of the Metallurgical Society of AIME 12 (1936) 244–260.
[35] G. Borelius, L.E. Larsson, Kinetics of precipitation in aluminum–zinc alloys, Arkiv foer Matematik, Astronomi och Fysik 35A (13) (1948) 1–14.
[36] A. Meunster, K. Sagel, Miscibility gap and critical point of the aluminum–zinc system, Zeitschrift fuer Physikalische Chemie 7 (1956) 267–295.
[37] L.E. Larsson, Pre-precipitation and precipitation phenomena in the Al–Zn system, Acta Metallurgica 15 (1967) 35–44.
[38] M. Simerska, P. Bartuska, The X-ray diffraction and electron microscopic investigation of stable and metastable equilibria in Al-rich Al–Zn alloys, Czech Journal of Physics B24 (1974) 553–559.
[39] H. Terauchi, N. Sakamoto, K. Osamura, Y. Murakami, Small angle X-ray critical scattering in an aluminum–zinc alloy with critical composition, Transactions of the Japan Institute of Metals 16 (7) (1975) 379–383.
[40] J.M. Holender, J. Soltys, The studies of the eutectoidal decomposition of Al–59 at.% Zn at the temperature close to the critical temperature, Diffusion and Defect Data–Solid State Data, Pt. A: Defect and Diffusion Forum 66–69 (1989) 1461–1466.
[41] W.M. Pierce, M.S. Palmerton, Studies on the constituent of binary zinc-based alloys, Transactions of the Metallurgical Society of AIME 68 (1923) 767–795.
[42] H. Auer, K.E. Mann, Magnetic investigation of the aluminum–zinc system, Zeitschrift fur Metallkunde 28 (1936) 323–326.
[43] M.L. Fuller, R.L. Wilcox, Phase changes during aging of zinc-alloy die castings, II—Changes in the solid solution of aluminum in zinc and their relation to dimensional changes, Transactions of the Metallurgical Society of AIME 122 (1936) 231–246.
[44] A. Burkhardt, Zinc alloys as a substitute material, Zeitschrift fur Metallkunde 28 (10) (1936) 299–308.
[45] K. Lohberg, X-ray determination of the solubility of aluminum and copper in zinc, Zeitschrift fur Metallkunde 32 (1940) 86–90.
[46] W. Hoffman, G. Fahrenhost, Precipitation rates in high purity zinc–aluminum and zinc–copper alloys, Zeitschrift fur Metallkunde 42 (1950) 460–463.
[47] A. Pasternak, The solid solubility of metals in lead and zinc, Bulletin International de l'Academie Polonaise des Sciences et des Lettres, Classe des Sciences Mathematiques et Naturelles, Serie A: Sciences Mathematiques Serial A (1951) 177–192.
[48] F.E. Wittig, G. Keil, Heats of mixing of binary liquid aluminum–B-metal alloys (zinc, cadmium, indium, thallium, tin, lead and bismuth), Zeitschrift fur Metallkunde 54 (10) (1963) 576–590.
[49] J.E. Hilliard, B.L. Averbach, M. Cohen, Thermodynamic properties of solid aluminum–zinc alloys, Acta Metallurgica 2 (1954) 621–631.
[50] H. Corsepius, A. Munster, On the thermodynamic properties of solid aluminum–zinc alloys, Zeitschrift fuer Physikalische Chemie 22 (1959) 1–19.
[51] R.E. Wittig, L. Schoffl, Heat of formation in the aluminum–zinc system at 330, 370 and 430°C, Zeitschrift fur Metallkunde 51 (1960) 700–707.
[52] R.A. Connell, D.B. Downie, The enthalpies of formation of α-phase Al–Zn alloys, Metal Science Journal 7 (1973) 12–14.
[53] G. Batalin, E.A. Beloborodova, The activity of Al in the liquid, Russian Metallurgy 4 (1968) 121–125.
[54] B. Predel, U. Schallner, On the thermodynamic properties of binary aluminum alloys containing gallium and zinc, Zeitschrift fur Metallkunde 60 (11) (1969) 869–877.
[55] J. Sebkova, M. Beranek, Application of the EMF method for measurement of aluminum activities in liquid aluminum alloys, Sbornik Vysoke Skoly Chemicko-Technologicke v Praze, B: Anorganicka Chemie a Technologie B18 (1974) 217–225.
[56] G.J. Lutz, A.F. Voigt, A radioactive tracer dew point method for measuring vapor pressures of binary alloys, the zinc–aluminum system, Journal of Physical Chemistry 67 (12) (1963) 2795–2799.
[57] P. Bolsaitis, P.M. Sullivan, The activity of zinc in liquid Zn–Al alloys from isopietic measurements, Transactions of the Metallurgical Society of AIME 245 (1969) 1435–1438.
[58] A. Yazawa, Y.K. Lee, Thermodynamic studies of the liquid aluminum alloy systems, Transactions of the Japan Institute of Metals 11 (6) (1970) 411–418.
[59] W. Ptak, L. Zabdyr, Determination of thermodynamic properties of aluminum–zinc solid solutions by EMF measurements, Archiwum Hutnictwa 16 (3) (1971) 253–267.
[60] R.E. Miller, J.L. Straalsund, D.B. Masson, The effect of electron concentration on the thermodynamic properties of two alloy phases in the Al–Zn–Ag system, Metallurgical Transactions 3 (1971) 545–550.
[61] V. Piacente, V.D. Paolo, G. D'Ascenzo, The activity of zinc in solid Al–Zn alloys, Thermochimica Acta 16 (1976) 63–68.
[62] T. Takahashi, N. Asano, Thermodynamic studies of solid aluminum–zinc alloys, Niihama Kogyo Koto Senmon Gakko Kiyo, Rikogaku-hen 18 (1982) 78–84.

Please cite this article in press as: S. Wasiur-Rahman, M. Medraj, A thermodynamic description of the Al–Ca–Zn ternary system, CALPHAD: Computer Coupling of Phase Diagrams and Thermochemistry (2009), doi:10.1016/j.calphad.2009.06.001

[63] O. Redlich, A.T Kister, Thermodynamics of nonelectrolyte solutions, *X–Y–T* relations in a binary system, Journal of Industrial and Engineering Chemistry Washington DC 40 (1948) 341–345.
[64] D. Kevorkov, R. Schmid-Fetzer, The Al–Ca system, Part 1; experimental investigation of phase equilibria and crystal structures, Zeitschrift fur Metallkunde 92 (2001) 946–952.
[65] K. Ozturk, L.Q. Chen, Z.-K. Liu, Thermodynamic assessment of the Al–Ca binary system using random solution and associate models, Journal of Alloys and Compounds 340 (1–2) (2002) 199–206.
[66] N. Kono, Y. Tsuchida, S. Muromachi, H. Watanabe, Study of the Al–Ca–Zn ternary phase diagram, Light Metals 35 (1985) 574–580.
[67] A.F. Messing, M.D. Adams, R.K. Steunenberg, Contribution to the phase diagram calcium–zinc, Transactions of the ASM. 56 (1963) 345–350.
[68] V.P. Itkin, C.B. Alcock, The Ca–Zn system, Bulletin of Alloy Phase Diagrams 11 (4) (1990) 328–333.
[69] G. Cordier, E. Czech, H. Schafer, $CaAl_2Zn_2$, the first example of an inverse $ThCr_2Si_2$ structure, Zeitschrift fuer Naturforschung, Teil B: Anorganische Chemie, Organische Chemie 39B (12) (1984) 1629–1632.
[70] A. Prince, The Al–Ca–Zn system, Bulletin of Alloy Phase Diagrams 10 (5) (1989) 540–545.
[71] A.T. Dinsdale, Thermodynamic data for the elements, CALPHAD 15 (4) (1991) 317–425.
[72] P.J. Spencer, A.D. Pelton, Y-B. Kang, P. Chartrand, C.D. Fuerst, Thermodynamic assessment of the Ca–Zn, Sr–Zn, Y–Zn and Ce–Zn system, CALPHAD 32 (2) (2008) 423–431.
[73] F. Sommer, Association model for the description of thermodynamic functions of liquid alloys II. Numerical treatment and results, Zeitschrift fuer Metallkunde 73 (2) (1982) 77–86.
[74] A.D. Pelton, Y-B. Kang, Modeling short-range ordering in solutions, International Journal of materials Research 98 (2007) 1–10.
[75] A.D. Pelton, S.A. Degterov, G. Eriksson, C. Robelin, Y. Dessureault, The modified quasi-chemical model I – Binary solutions, Metallurgical and Materials Transactions B 31B (2000) 651–659.
[76] A.D. Pelton, P. Chartrand, The modified quasi-chemical model: Part II. Multicomponent solutions, Metallurgical and Materials Transactions A 32A (2001) 1355–1360.
[77] P. Chartrand, A.D. Pelton, The modified quasi-chemical model: Part III. two sublattices, Metallurgical and Materials Transactions A 32A (2001) 1397–1407.
[78] P.S. Rudman, B.L. Averbach, X-ray measurements of local atomic arrangements in aluminum–zinc and in aluminum–silver solid solutions, Acta Metallurgica 2 (1954) 576–582.
[79] G.W. Toop, Predicting ternary activities using binary data, Transactions of The American Institute of Mining 233 (5) (1965) 850–855.
[80] H. Okamoto (Ed.), Binary Alloy Phase Diagrams, ASM, 1996, (second edition plus updates).
[81] K. Ozturk, Y. Zhong, L-Q. Chen, C. Wolverton, J.O. Sofo, Zi-Kui Liu, Linking first-principles energetics to CALPHAD: An application to thermodynamic modeling of the Al–Ca binary system, Metallurgical and Materials Transactions A 36A (1) (2005) 5–13.
[82] M.L. Fornasini, F. Merlo, $CaZn_3$: A structure with mixed $BaLi_4$ and $CeCu_2$-like ordering, Acta Crystallography B36 (8) (1980) 1739–1744.
[83] G. Bruzzone, E. Franceschi, F. Merlo, M_5X_3 intermediate phases formed by Ca, Sr and Ba, Journal of the Less-Common Metals 60 (1978) 59–63.
[84] J. Wieting, Crystal structure of $CaZn_2$, Naturwissenschaften 48 (1961) 401.
[85] W. Haucke, The crystal structure of $CaZn_5$ and $CaCu_5$, Zeitschrift Fuer Anorganische Chemie 244 (1940) 17–22.
[86] A. Iandelli, A. Palenzona, Zinc-rich phases of the rare-earth zinc alloys, Journal of the Less-Common Metals 12 (5) (1967) 333–343.
[87] J.A.A. Ketelaar, The crystal structure of alloys of zinc with the alkali and alkaline earth metals and of cadmium with potassium, Journal of Chemical Physics 5 (1937) 668.
[88] K. Matsuyama, On the equilibrium diagram of the Al–Ca system, Science Reports of the Tohoku Imperial University 17 (1928) 783–789.
[89] L. Donski, Alloys of Ca with Zn, Al, Ti, Pb, Sn, Bi, Sb and Cu, Zeitschrift Anorganische und Allgemeine Chemie 57 (1908) 201–205.
[90] F. Sommer, J.J. Lee, B. Predel, Thermodynamic investigation of liquid Al–Ca, Al–Sr, Mg–Ni and Ca–Ni alloys, Zeitschrift fur Metallkunde 74 (1983) 100–104.
[91] Y.O. Esin, V.V. Litovskii, S.E. Demin, M.S. Petrushevski, Heats of formation of liquid alloys of aluminum with strontium and barium with silicon, Zhurnal Fizicheskoi Khimii 59 (3) (1985) 768–769.
[92] K.T. Jacob, S. Srikanth, Y. Waseda, Activities, concentration fluctuations and complexing in liquid Ca–Al alloys, Transactions of the Japan Institute of Metals 29 (1988) 50–59.
[93] E. Schürmann, C.P. Fünders, H. Litterscheidt, Vapor pressure of Ca above Ca–Si, Ca–Al and Ca–Al–Si alloys, Archiv fur das Eisenhuttenewsen 46 (1975) 473–476.
[94] D. Kevorkov, R. Schmid-Fetzer, A. Pisch, F. Hodaj, C. Colinet, The Al–Ca system, Part 2: Calorimetric measurements and thermodynamic assessment, Zeitschrift fur Metallkunde 92 (2001) 953–958.
[95] M. Notin, J.C. Gachon, J. Hertz, Enthalpy of formation of Al_4Ca and Al_2Ca and of the liquid alloys (Aluminum + Calcium), Journal of Chemical Thermodynamcis 14 (5) (1982) 425–434.
[96] M. Notin, J. Hertz, Thermodynamic data for calcium-based alloys from a new galvanic method, CALPHAD 6 (1) (1982) 49–56.
[97] E. Velesckis, Application of hydrogen titration method to a thermodynamic investigation of solid Al–Ca alloys, Journal of Less-Common Metals 80 (2) (1981) 241–255.

Please cite this article in press as: S. Wasiur-Rahman, M. Medraj, A thermodynamic description of the Al–Ca–Zn ternary system, CALPHAD: Computer Coupling of Phase Diagrams and Thermochemistry (2009), doi:10.1016/j.calphad.2009.06.001